

## Development of a novel antifouling polyethersulfone composite membrane with PHEMA-b-F127-b-PHEMA as an additive for oil-in-water emulsion separation

Jun Yin, Xinan Cai, Meng Chen\*

Department of Biological and Chemical Engineering, Jing De Zhen University, Jing De Zhen 333000, Jiangxi, China,  
email: 364278215@qq.com (M. Chen)

Received 20 March 2020; Accepted 15 April 2021

### ABSTRACT

Pluronic F127-block-poly(2-hydroxyethyl methacrylate) (PHEMA-b-F127-b-PHEMA) was beforehand synthesized via the RAFT polymerization and used as an additive with polyethersulfone (PES) matrix to fabricate composite membranes by the phase inversion method. During the membrane formation process, the highly hydrophilic PHEMA blocks migrate spontaneously onto the membrane surfaces, which can be verified by the attenuated total reflectance-Fourier transform infrared spectroscopy. As a result, the composite membrane surface porosity and hydrophilicity were enhanced compared with the unmodified PES membrane. More importantly, the water permeability and anti-fouling ability of composite membranes were improved significantly. Furthermore, the PHEMA blocks enriched on the as-made PES composite membrane surface, which acted as an anchor to immobilize the initiating site. Therefore, a lot of functional polymers were effectively grafted onto the PES composite membranes by surface-initiated radical polymerization.

**Keywords:** Polyethersulfone membrane; 2-hydroxyethyl methacrylate; Antifouling property; Pluronic F127

### 1. Introduction

Every day, a large amount of oily wastewater is generated by many industrial processes, resulting in terrible environmental pollution and resource utilization problems. Hence, cost-effective technologies must be developed to treating oily wastewater. Conventional treatment methods including gravity separation and skimming, photocatalytic treatment, de-emulsification, centrifugation and dissolved air flotation have been developed for the application of oily wastewater separation [1–2]. However, there are many drawbacks such as high energy consumption, low operation efficiency, and secondary contamination problems [3]. What's important is that these traditional methods are not effective for treating the surfactant-stabilized oil-in-water emulsions, where oil droplets are stably dispersed in water under the interaction of

surfactants. Hence, new advanced separation technologies for oil-in-water emulsion must be developed.

The application of several kinds of membrane separation technologies for treating oil-in-water emulsion have increasingly become a viable alternative method due to their low energy requirement, high operation efficiency and negligible environmental pollution when compared to the traditional methods [4–7]. Among the predominant membrane material used in membrane technology, polyethersulfone (PES) has drawn much attention, which possesses outstanding membrane-forming properties, as well as mechanical strength and chemical and thermal stability [8–10]. However, the PES membrane is typically lacks of hydrophilicity often causes the adsorption and deposition of oil droplets on the PES membrane surface, which leads to serious membrane fouling and rapid decline of permeation flux in oil-in-water separation. It is generally acknowledged

\* Corresponding author.

that increasing the membrane surface hydrophilicity can improve remarkably membrane antifouling ability [10].

Accordingly, the commonly used modification methods such as surface coating, physical blending, surface grafting, and modification of membrane bulk materials have been performed to improve the hydrophilicity of PES membrane [11–18]. Much researches have been published about the successes in improving the antifouling property of PES membranes. Nevertheless, these traditional modification methods exist various disadvantages. For example, in surface coating, the hydrophilic coating susceptible to leach from the membrane, which reduces the lifespan of membrane [12]. Chemical modification of bulk materials often results in a decrease in membrane mechanical strength. In surface grafting, additional surface treatments such as plasma excitation, UV or high energy irradiation, ozone treatment are often applied to obtain reactive sites on inert membrane surface [14,16,17]. These methods are difficult to popularize due to the complicated process and high energy consumption. Therefore, more efficient strategies for hydrophilization modification of PES membranes are urgently needed.

Very recently, amphiphilic copolymers have been designed as additives in the fabrication of ultrafiltration membranes [19–25]. The hydrophobic segments are often required to be well miscible with the hydrophobic membrane bulk materials, whereas the hydrophilic segments migrate toward the membrane surface to minimize the interfacial free energy during the immersion precipitation process. As a result, the hydrophilic chains are tightly tethered onto the membrane surface by the entanglements between hydrophobic chains and membrane bulks, which endow the fabricated membranes with long-term stable hydrophilicity. Additionally, if the hydrophilic chains in amphiphilic copolymers contain reactive groups, the composite membrane surface can be further functionalized via numerous chemical modifications participated by these reactive groups [19–21].

Inspired by these works, herein a novel block copolymer (PHEMA-*b*-F127-*b*-PHEMA) is designed as a hydrophilic additive, has been successfully synthesized by the grafting hydrophilic PHEMA chain onto the F127 molecular. Then the composite membranes were fabricated by wet phase inversion. The effects of additive dose on membrane properties such as porosity, permeability and surface hydrophilicity of fabricated membranes were investigated. Moreover, the antifouling properties and fouling resistances of the membranes were also researched in detail.

## 2. Experimental

### 2.1. Materials

Polyethersulfone (PES Mw = 150,000 g/mol) was supplied by JiDa High Performance Materials Co., Ltd. and was dried at 100°C for at least 12 h before use. Pluronic F127 (Mn = 12,600 g/mol) was purchased from Sigma and recrystallized before use, 2-hydroxyethyl methacrylate (HEMA, 98%) was brought from Aladdin and passed through a basic alumina column to remove the inhibitor,

4-dimethylaminopyridine (DMAP), 2,2'-azobisisobutyronitrile (AIBN, 98%), 1-ethyl-3-[3-dimethylaminopropyl] carbodiimide hydrochloride (EDCI), sodium dodecyl sulfate (SDS, 99%) used without further purification, dimethylacetamide (DMAc), 1,4-dioxane and methylene chloride (DCM) were purified by distillation from CaH<sub>2</sub>. Engine oil (20 W–40) was purchased from Exxon Mobil Oil Company.

### 2.2. Synthesis of PHEMA-*b*-F127-*b*-PHEMA

The synthetic routes of PHEMA-*b*-F127-*b*-PHEMA were presented in Fig. 1 and described in the following steps.

#### 2.2.1. Synthesis of macro RAFT agent (CPADB-F127-CPADB)

The RAFT agent, (4-cyanopentanoic acid dithiobenzoate, CPADB) was synthesized using a previously published method [26]. Then, Pluronic F127 (8.0 g, 16.8 mmol), DMAP (27.2 mg, 0.16 mmol), EDCI (230.4 mg, 1.2 mmol), CPADB (232.0 mg, 0.8 mmol) and 1,4-dioxane (60 mL) were charged into a round-bottomed flask, which was capped and degassed with nitrogen for 1 h at 25°C. The solution was stirred for 24 h at 60°C, and subsequently, the solvent was removed. The viscous product was dissolved in 60 mL of anhydrous DCM, and the solution was extracted with a saturated NaHCO<sub>3</sub> solution, followed by water and saturated NaCl solution and then dried over anhydrous MgSO<sub>4</sub>. After evaporation of the solvent, the final red viscous product was purified by precipitating from diethyl ether.

#### 2.2.2. RAFT polymerization of HEMA with the CPADB-F127-CPADB

For the RAFT polymerization of HEMA, 5.2 g (40.0 mmol) of HEMA, 13.2 mg (0.08 mmol) of AIBN, 5.3 g (0.4 mmol) of CPADB-F127-CPADB and 30 mL 1,4-dioxane were introduced to a Schlenk tube. The tube was subjected to three freeze-pump-thaw cycles to remove oxygen. The polymerization was carried out in an oil bath preheated to 60°C for 12 h. Then the polymerization was quenched by putting the tube into ice water. After removal of the 1,4-dioxane, the viscous product was dialyzed at room temperature using a cellulose membrane (MW 8,000 g/mol) for 48 h.

### 2.3. PES composite membrane preparation

The composite membranes were prepared with PES as bulk material, PHEMA-*b*-F127-*b*-PHEMA as the blend additive, DMAc as the solvent, and deionized water (25°C) as the coagulant, respectively. PHEMA-F127-PHEMA (2, 5, and 10 wt.% relative to the weight of PES) and PES were dissolved into DMAc at 50°C for 24 h to obtain a homogeneous casting suspension, after bubble removal, the blend solution was cast on a clean glass and quickly immersed into water at 25°C. The fabricated PES/ PHEMA-*b*-F127-*b*-PHEMA membranes were named as M2, M5, and M10 according to the weight percentage

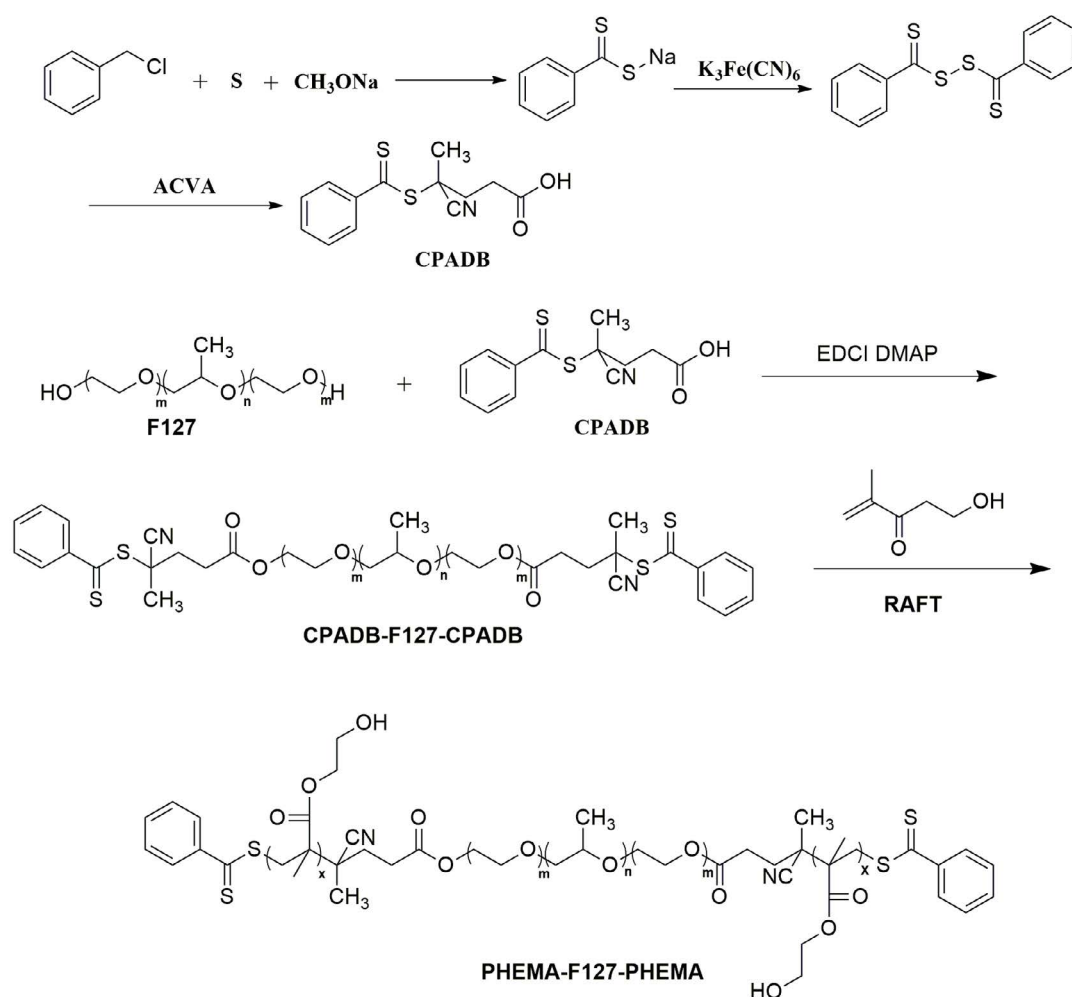


Fig. 1. Synthesis route of PHEMA-F127-PHEMA via RAFT polymerization.

of PHEMA-*b*-F127-*b*-PHEMA. By contrast, the PES/F127 composite membranes with the same amount of F127 were also prepared through identical conditions, named as m2, m5, and m10 respectively. The neat PES membrane with 0 wt.% additive was fabricated as the blank membrane. The compositions of the casting solution were shown in Table 1.

#### 2.4. Characterization of PHEMA-*b*-F127-*b*-PHEMA and membranes

The Fourier transform infrared spectroscopy spectra (FTIR, Bruker Tensor 27) was used to analyze the chemical composition of F127, F127-CPADB, PHEMA-*b*-F127-*b*-PHEMA. <sup>1</sup>H NMR spectra were measured in deuterated chloroform (CDCl<sub>3</sub>) for CPADB and deuterated dimethyl sulfoxide (DMSO-*d*<sub>6</sub>) for PHEMA-*b*-F127-*b*-PHEMA on Bruker AV300 MHz. Number-average molecular weights and the polydispersity indices were measured on PL-GPC 220 system, DMF was used as the mobile phase at a flow rate of 1 mL min<sup>-1</sup>. The surface chemistry of the fabricated membranes was confirmed by attenuated total reflectance-Fourier transform infrared spectroscopy (ATR-FTIR).

The membrane porosity was measured by the gravimetric method [4,27]. The porosity ( $\epsilon$ , %) of the membrane was calculated according to Eq. (1):

$$\epsilon = \frac{(m_w - m_d)}{AL\rho} \times 100\% \quad (1)$$

where  $m_w$ ,  $A$ ,  $L$  are the wet membrane weight (g), effective area (cm<sup>2</sup>) and thickness (cm),  $m_d$  is the dry membrane weight (g), and  $\rho$  is the pure water density (g/cm<sup>3</sup>), respectively. All measurements were repeated three times and the average values were calculated to minimize experimental error.

The static water contact angle was measured using a contact angle measurement instrument (JC-2000C1) to reveal the surface hydrophilicity of fabricated membranes. Deionized water was dropped randomly on the surface of the membrane sample at five locations, and the average value was obtained.

BSA was used as a model protein to evaluate the anti-fouling ability of fabricated membranes. Each tested membrane was rinsed with buffer solution (0.1 M PBS, pH = 7.4).

Table 1  
Composition of casting solutions for preparation of the PES composite membranes

Membrane	PES (wt.%)	Additive (wt.%)	DMAc (wt.%)
PES	15	0	85.00
PES/F2 (m2)	15	0.30 F127	84.70
PES/F5 (m5)	15	0.75 F127	84.25
PES/F10 (m10)	15	1.50 F127	83.50
PES/FH2 (M2)	15	0.30 PHEMA-F127-PHEMA	84.70
PES/FH5 (M5)	15	0.75 PHEMA-F127-PHEMA	84.25
PES/FH10 (M10)	15	1.50 PHEMA-F127-PHEMA	83.50

The treated membrane was immersed into 20 mL of BSA solution (0.2 g L<sup>-1</sup>, pH = 7.4) in an airtight glass bottle and shaken in darkness at 25°C for 24 h. The amount of adsorbed BSA was calculated from the concentrations of BSA in the solution before and after BSA adsorption.

### 2.5. Oil-in-water emulsion preparation

Engine oil (20 W–40) and SDS were added to deionized water, the mass ratio of oil and SDS was 9:1, and oil concentration was 0.9 g/L. Then the mixture was dispersed by a high-shear dispersion homogenizer for 30 min to obtain a steady oil-in-water emulsion.

### 2.6. Membrane Performance Characterization

A dead-end stirred cell (CB-380) filtration system was used to survey the permeate flux of the prepared membranes. The tests were carried out at 25°C ± 1°C with a stirring speed of 400 rpm. The detailed procedure consisted of the following steps: (1) each test membrane was initially pressurized at 0.15 MPa for 0.5 h, then, the pressure was decreased to 0.1 MPa and the stable pure water flux (PWF) was obtained as  $J_{w1}$ ; (2) then, oil-in-water emulsion (0.9 g/L) was permeated through the test membrane. After 1 h of oil-in-water emulsion filtration, the oil flux was obtained as  $J_{oil}$ ; (3) after that, the fouled membranes were washed with deionized water for about 30 min; (4) finally, the pure water flux ( $J_{w2}$ ) of the cleaned membrane was obtained according to the first step. The  $J_{w1}$ ,  $J_{oil}$ ,  $J_{w2}$  (L/m<sup>2</sup>h) were calculated by Eq. (2):

$$J = \frac{V}{At} \quad (2)$$

where  $V$  (L),  $t$  (h),  $A$  (cm<sup>2</sup>) are the volume of permeated water, the filtration time, the effective membrane area, respectively. The oil concentrations of the permeate solution ( $C_p$ ) and the feed solution ( $C_f$ ) were measured by spectrophotometer at 531 nm wavelength. The oil rejection,  $r$  was calculated according to the following expression:

$$r = \left( 1 - \frac{C_p}{C_f} \right) \times 100\% \quad (3)$$

To evaluate the antifouling ability of the as-prepared membrane, flux recovery ratios (FRR) was calculated by the following equation [4,27]:

$$FRR = \frac{J_{w2}}{J_{w1}} \times 100\% \quad (4)$$

The reversible fouling ( $R_r$ ), irreversible fouling ( $R_{ir}$ ) and total fouling ( $R_t$ ) can be obtained by the following equations [4,27]:

$$R_r = \left( \frac{J_{w2} - J_{oil}}{J_{w1}} \right) \times 100\% \quad (5)$$

$$R_{ir} = \left( \frac{J_{w1} - J_{w2}}{J_{w1}} \right) \times 100\% \quad (6)$$

$$R_t = R_r + R_{ir} = \left( \frac{J_{w1} - J_{oil}}{J_{w1}} \right) \times 100\% \quad (7)$$

## 3. Results and discussion

### 3.1. Characteristics of synthesized polymer additives PHEMA-b-F127-b-PHEMA

The synthetic route for preparing PHEMA-b-F127-b-PHEMA is depicted in Fig. 1. As can be seen, the RAFT agent, CPADB is synthesized using a previously published method [26]. Then, the F127-CPADB acting as a macro chain transfer agent is synthesized via the esterification reaction of CPADB and F127. The PHEMA-b-F127-b-PHEMA is prepared through reversible addition-fragmentation chain transfer (RAFT) polymerization.

FT-IR spectra for F127, F127-CPADB and PHEMA-b-F127-b-PHEMA are exhibited in Fig. 2. In the case of F127 (Fig. 2a), the typical peak associated with CH<sub>x</sub> stretching vibration is visible at around 2,900 cm<sup>-1</sup>. In contrast, a new weak peak at 1,735 cm<sup>-1</sup> appears (Fig. 2b), which is assigned to -C=O groups, indicating that the CPADB has been successfully graft to the F127. After RAFT polymerization, a strong peak around 3,400 cm<sup>-1</sup> due to O-H

stretching is observed which correlated with the structure of PHEMA, and the characteristic adsorption peak assigned to carbonyl (C=O) vibration is clearly visible at 1,735  $\text{cm}^{-1}$ , indicating the successful RAFT polymerization of PHEMA-b-F127-b-PHEMA.

The successful synthesis of CPADB is confirmed by  $^1\text{H}$  NMR analysis (Fig. 3). As shown in Fig. 3, the chemical shifts at 7.2–7.8 ppm are assigned to aromatic protons (d, e, f), the chemical shifts at 1.9 ppm could be ascribed to the protons of  $-\text{CH}_3-$  (c).

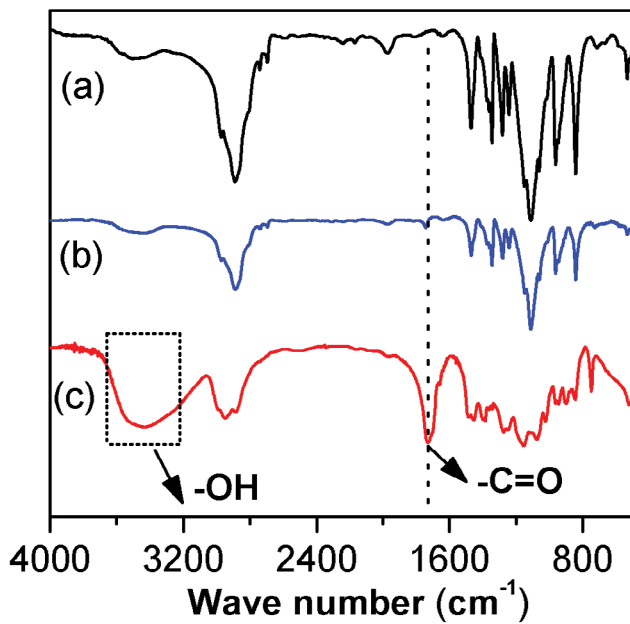


Fig. 2. FT-IR spectra of (a) F127, (b) F127-CPADB, and (c) PHEMA-F127-PHEMA.

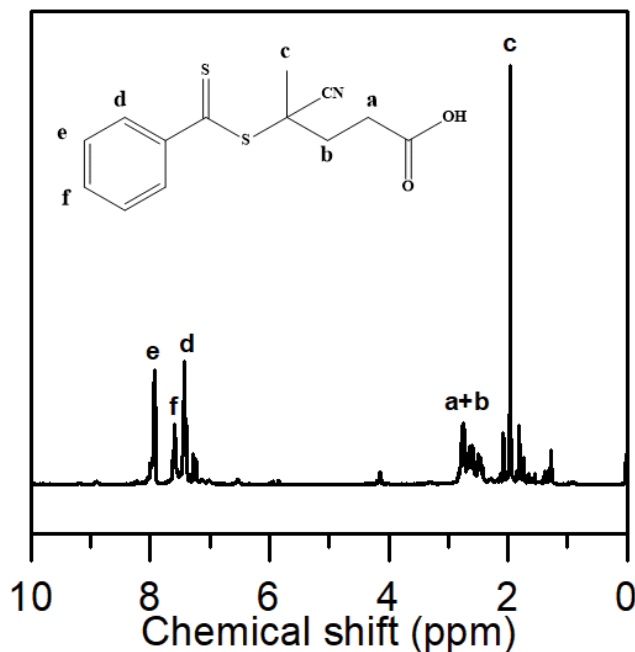


Fig. 3.  $^1\text{H}$ -NMR spectra of CPADB in  $\text{CDCl}_3$ .

Fig. 4 exhibits the  $^1\text{H}$  NMR spectra of PHEMA-F127-b-PHEMA. As shown in Fig. 4, the chemical shifts at 3.64, 3.88 and 4.86 ppm are assigned to the adsorption of  $-\text{O}-\text{CH}_2$  (c),  $-\text{CH}_2-\text{OH}$  (b) and  $-\text{OH}$  (a), the chemical shifts at 1.9 and 0.7 ppm could be ascribed to the protons of  $-\text{CH}_2-$  (d) and  $-\text{CH}_3$  (e) at the polymer main chains, indicating the successful synthesis of PHEMA-F127-PHEMA.

The number-average molecular weights ( $M_n$ ) and the polydispersity indices (PDI) of the F127 and PHEMA-b-F127-b-PHEMA, deduced from GPC are listed in Fig. 5.

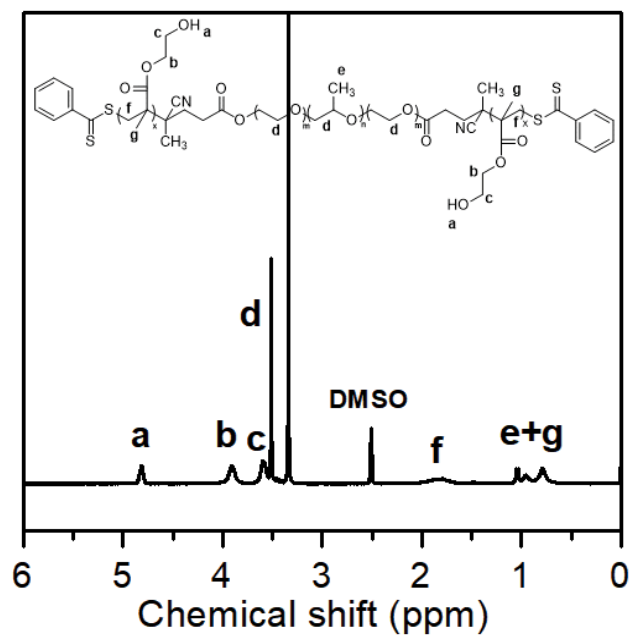


Fig. 4.  $^1\text{H}$ -NMR spectra of PHEMA-F127-PHEMA in  $\text{DMSO-d}_6$ .

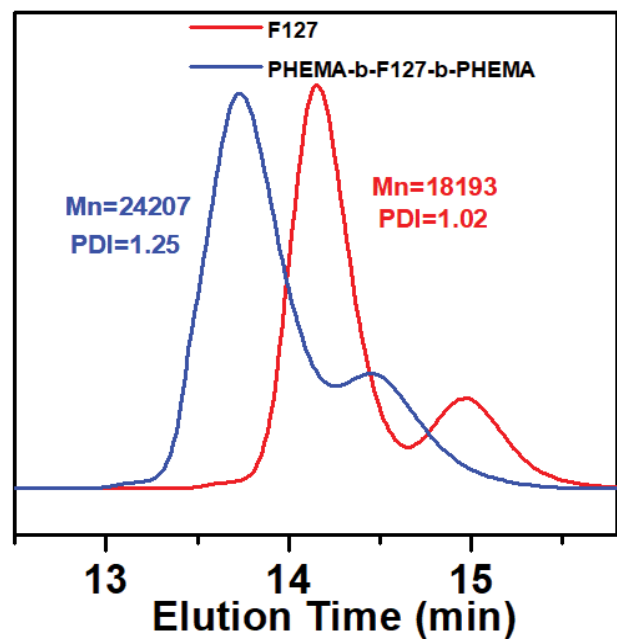


Fig. 5. GPC spectra for F127 and PHEMA-b-F127-b-PHEMA.

Clearly, the  $M_n$  of the PHEMA-b-F127-b-PHEMA is determined to be 24,207 g/mol and molecular weight distributions remained narrow (PDI = 1.25), this indicates a controlled polymerization. Combined with the analysis of FTIR,  $^1\text{H}$  NMR and GPC, it is reasonable to assume that the PHEMA-b-F127-b-PHEMA has been successfully synthesized.

### 3.2. Surface-segregation of PHEMA blocks on the membrane matrix surface

In this work, PPO is designed as the hydrophobic segments of the amphiphilic additive used for the modification of PES membranes. The PPO backbones in the PHEMA-b-F127-b-PHEMA are amalgamated with PES molecular and act as an anchor of PHEMA chains. The enrichment of PHEMA chains on the membrane surface is confirmed by ATR-FTIR analysis. As shown in Fig. 6a, the pure PES membrane shows no adsorption peaks at  $3,400\text{ cm}^{-1}$  (O–H stretching) and  $1,735\text{ cm}^{-1}$  (carbonyl vibrations), while the signal are clearly visible for the PES/FH composite membrane (M5), and PHEMA is the only source of those adsorption peaks, indicating the successful surface-segregation of PHEMA blocks on membrane matrix surface.

### 3.3. Morphology of the membrane

The surface and cross-section morphologies of PES blank membrane and M5 composite membranes are observed. As shown in Fig. 7, all tested membranes exhibit

asymmetric structures, including a waferly dense top-layer, a porous finger-like sub-layer and fully developed macrovoid. The composite membranes have higher porosity and larger surface pore size than PES blank membrane.

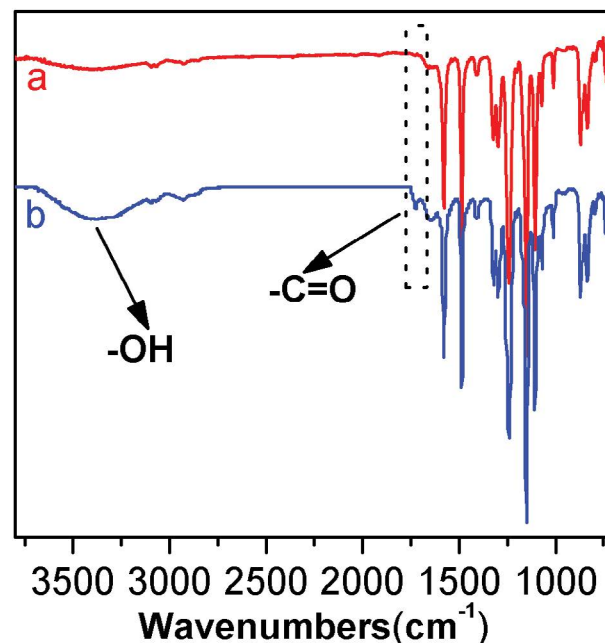


Fig. 6. ATR-FTIR spectra of (a) PES and (b) PES/FH5 membranes.

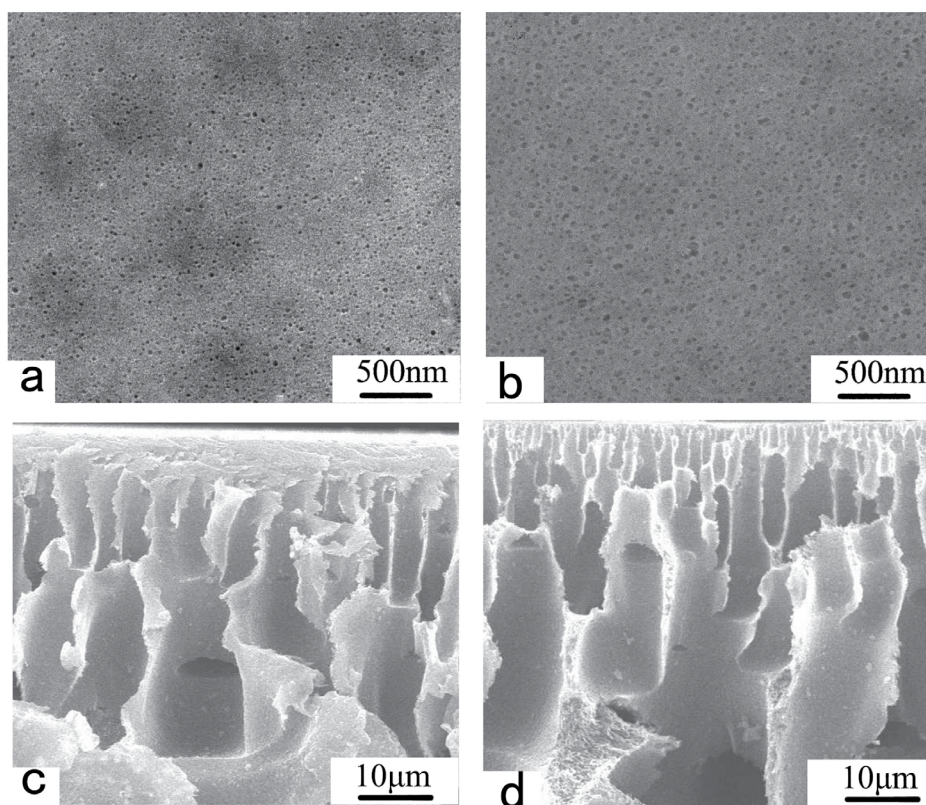


Fig. 7. Surface and cross-sectional morphologies of the PES (a, c) and M5 (b, d) membranes.

Moreover, quantitative calculation results of porosity are shown in Fig. 8, which will discuss in detail in the following sections. There are no appreciable cross-sectional morphological variations between the PES membrane and M5 composite membrane.

### 3.4. Porosity and hydrophilicity of as-prepared membrane

The porosity of as-prepared membranes is quantitatively calculated and listed in Fig. 8. It could be seen that the porosity of membranes increases initially with the addition of a low amount of F127 and PHEMA-b-F127-b-PHEMA. Then, they reach the maximum when the F127 and PHEMA-b-F127-b-PHEMA dosage is 5 wt.%. However, they tend to decrease with the further increase the additive content, which is similar to other researches and would be explained by the following reasons: (1) thermodynamic stability of the casting solution would decrease after blending with the hydrophilic polymer, which results in the phase separation is happened at a relatively low polymer concentration [28]. As a result, the membrane having high surface porosity; (2) when the additive content is relatively high, the increased viscosity of the casting solution would significantly slow the exchange of DMAC and water as well as suppressed the formation of large pore size. As we know, the thermodynamic enhancement and rheological hindrance have the opposite effect on the porosity of as-prepared membranes. At a low additive concentration (2 wt.%, 5 wt.%), the thermodynamic enhancement played a dominant role, endowing the membrane high porosity. In the contrary, at a high additive concentration (10 wt.%), membranes with low porosity are obtained, which is attributed to the rheological hindrance that resulted from the increased viscosity of the casting solution.

Fig. 9 shows the water contact angle of the pristine PES membrane and PES/F, PES/FH composite membranes. The contact angle decreases from  $84.5^\circ \pm 1.5^\circ$  to  $77.4^\circ \pm 2.3^\circ$ ,

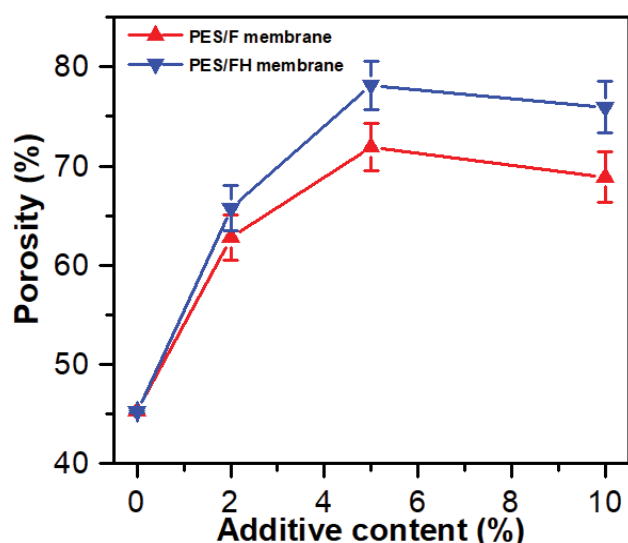


Fig. 8. Effect of additive content on porosity of PES/F and PES/FH composite membranes. Data were means  $\pm$  SD ( $n = 3$ ).

$66.4^\circ \pm 2.2^\circ$ , and  $63.9^\circ \pm 2.1^\circ$  respectively with the increase of F127 dosage, showing the better water affinity after the addition of the F127. Compared to the PES/F membranes, the PES/FH composite membranes present better hydrophilicity. Especially, the contact angle decreases to  $59.1^\circ \pm 3.6^\circ$  when the PHEMA-b-F127-b-PHEMA dosage is 10 wt.%. This may be attributed to the stronger interaction between PHEMA blocks and water, which could drive the hydrophilic chains to migrate toward the membrane surface to minimize the interfacial free energy during the immersion precipitation process.

### 3.5. Permeation and antifouling properties of as-prepared membrane

The antifouling ability of the membrane can be reflected by the protein (BSA) adsorption test. As everyone knows, lower amounts of BSA adsorbed on the membrane indicate the better antifouling ability of the membrane. The BSA adsorption results are shown in Fig. 10. The unmodified PES membrane displays the highest adsorption of BSA due to the hydrophobic nature of the PES materials, implying that the unmodified PES membrane is easily fouled by protein in water. The BSA adsorption amount of modified composite membranes is obviously lower than the PES membrane. Compared to the PES/F membranes, the PES/FH composite membranes have lower BSA adsorption amounts. This attributes to the better hydrophilicity of PES/FH composite membranes, which can effectively form a water molecule layer on the membrane surface and hinder the approach of protein. Therefore, the antifouling ability is noticeable.

Fig. 11 shows time-dependent flux for PES/F and PES/FH composite membranes. The test procedure consisted of the following steps: each membrane was initially pressurized at 1.6 bar for 1 h; Then, the operation pressure was reduced to 1.0 bar and the stable pure water flux (PWF) was measured as  $J_{w1}$ ; the feed liquid was changed to the oil-in-water emulsion, after 1 h filtration, the average oil flux

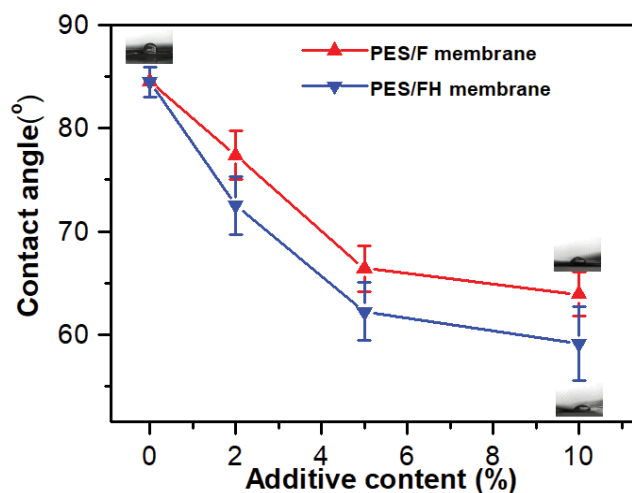


Fig. 9. Effect of additive content on static water contact angle of PES/F and PES/FH composite membranes. Data were means  $\pm$  SD ( $n = 3$ ).

was recorded as  $J_{oil}$ ; after that, the fouled membrane was rinsed with deionized water for about 30 min (not shown in Fig. 11); finally, the stable pure water flux ( $J_{w2}$ ) of cleaned membrane was obtained.

The pristine PES membrane exhibited the lowest PWF around 64.10 L/m<sup>2</sup> h, after the addition of F127 and PHEMA-b-F127-b-PHEMA, the PWF significantly increases at first, the flux of M5 reached to a maximum, which is about 5.1 times than that of the pristine PES membrane. As we know, the permeation flux was mainly determined by the hydrophilicity and porosity of the membrane. When 2, 5 wt.% additive was introduced into the casting solution, there were relatively high porosity (as shown in Fig. 8) compared to the pristine PES membrane

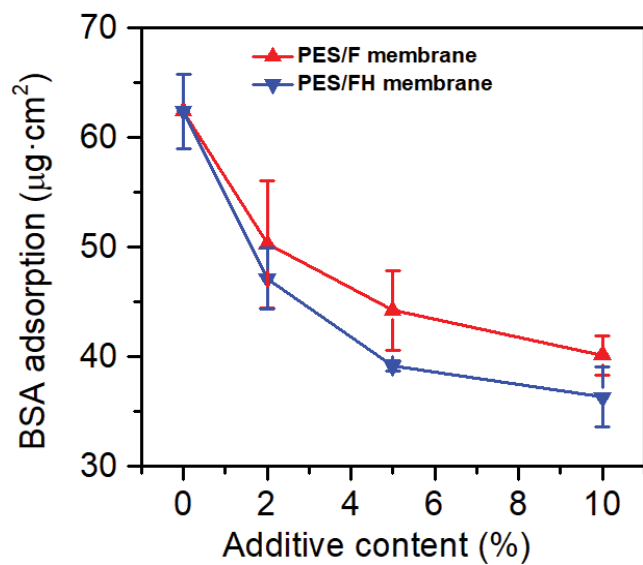


Fig. 10. BSA adsorption of PES/F and PES/FH composite membranes.

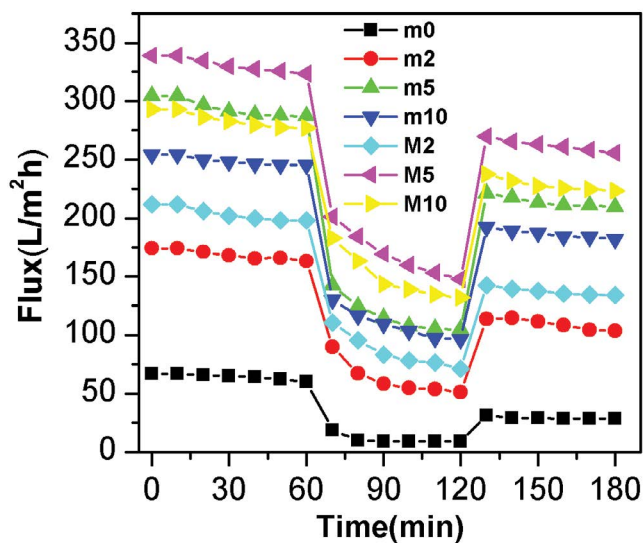


Fig. 11. Time-dependent flux for PES/F and PES/FH composite membranes with different content.

and enhanced hydrophilicity (as seen in Fig. 5) exhibited pure water flux of 168.02, 292.37 (m2,m5) and 202.71, 329.72 L/m<sup>2</sup> h (M2,M5). Interestingly, the values decreased with the further increase of the additive (10 wt.%). Since the hydrophilicity of m10 and M10 were higher than other membranes, the improved hydrophilicity could promote water molecules to pass through effectively the membrane pores, which would increase permeation flux [29,30]. But the flux is inconsistent with the hydrophilicity, this may be caused by the influence of the porosity was more significant.

After filtration of pure water, the oil-in-water emulsion was permeated through the test membrane.

The oil rejection of the PES blank membrane and composite membranes was 100%, indicating excellent oil removal efficiency, which can be confirmed by Fig. 12. For all test membranes, the flux behaved similarly and reduced sharply in few minutes of ultrafiltration, which was attributed to filtration cake formation by oil adsorption and deposition on the membrane surface [7]. After the dynamic balance between the deposition and re-suspension of oil droplets was reached, a relatively steady flux was obtained. It was worth noting that the PES/FH composite membranes (M2, M5 and M10) had less flux decrease than other membranes (PES, m2, m5 and m10). The membrane with more hydrophilicity, the less decrease for the flux. After 30 min rinsing the fouled membranes, the PWF of the washed membranes was recovered in different degrees.

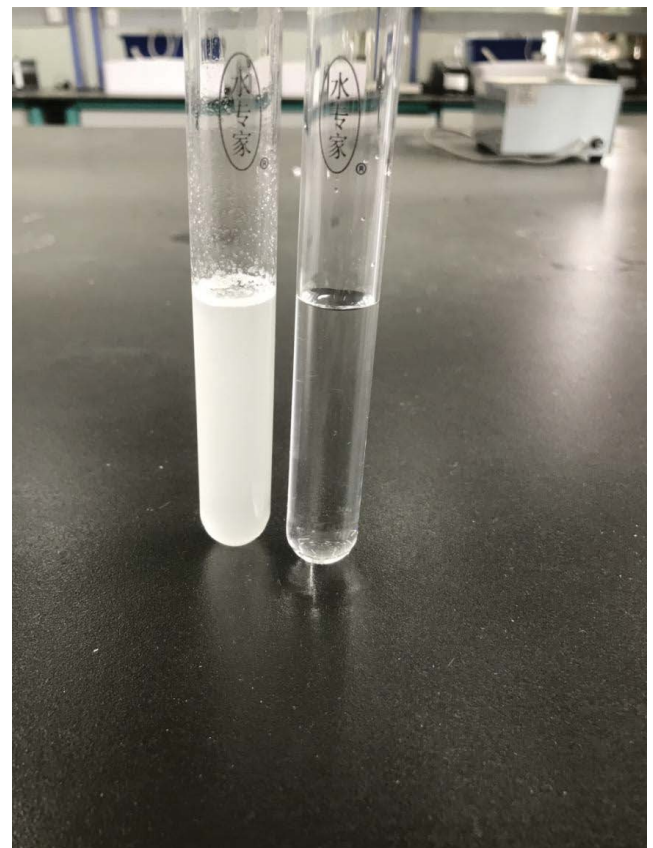


Fig. 12. The optical images of solution before and after separation of M5 membrane.

Table 2  
Summary of the corresponding fouling parameters of PES, PES/F and PES/FH membranes

Membrane	$R_i$ (%)	$R_{ir}$ (%)	$R_r$ (%)	$R_{ir}/R_i$ (%)	$R_r/R_i$ (%)
$m_0$	$82.70 \pm 0.60$	$54.25 \pm 0.36$	$28.45 \pm 0.44$	$65.60 \pm 1.17$	$34.40 \pm 2.52$
$m_2$	$62.81 \pm 2.36$	$35.01 \pm 2.52$	$27.80 \pm 1.45$	$55.74 \pm 3.06$	$44.26 \pm 1.85$
$m_5$	$58.20 \pm 1.95$	$26.81 \pm 3.37$	$31.39 \pm 1.38$	$46.07 \pm 3.61$	$53.93 \pm 3.28$
$m_{10}$	$56.16 \pm 1.60$	$24.77 \pm 3.11$	$31.39 \pm 1.22$	$44.11 \pm 1.30$	$55.89 \pm 2.51$
$M_2$	$57.67 \pm 1.01$	$32.32 \pm 1.31$	$25.35 \pm 3.99$	$56.05 \pm 1.90$	$43.95 \pm 1.57$
$M_5$	$48.66 \pm 2.72$	$20.46 \pm 1.42$	$28.20 \pm 1.34$	$42.05 \pm 1.05$	$57.95 \pm 2.45$
$M_{10}$	$47.20 \pm 2.66$	$19.18 \pm 1.64$	$28.02 \pm 3.09$	$40.64 \pm 2.01$	$59.36 \pm 2.34$

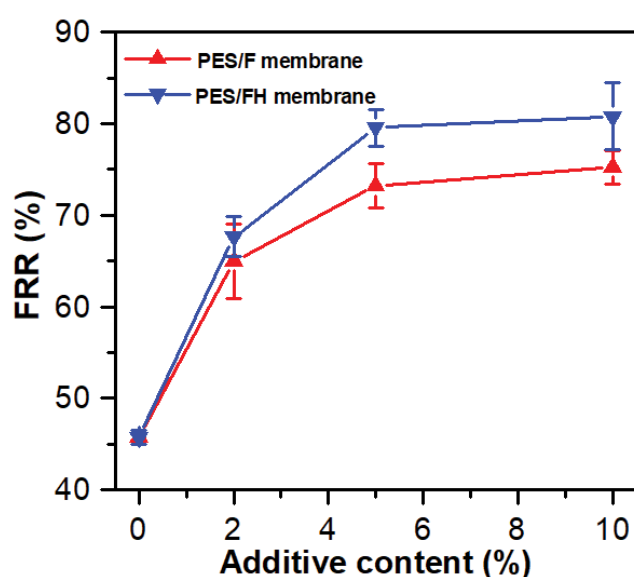


Fig. 13. Effect of additive content on water flux recovery ratio (FRR) of PES/F and PES/FH membranes. Data were means  $\pm$  SD ( $n = 3$ ).

The flux recovery rate (FRR) was introduced to evaluate the surface modification, the FRR value was obtained according to Eq. (5) and the results are exhibited in Fig. 13, the higher the FRR value, the better antifouling property of the membrane. Clearly, the FRR of M membranes (67.68%, 79.54% and 80.82% for M2, M5 and M10, respectively) were higher compared to the m membranes (64.99%, 73.19%, and 75.23% for m2, m5 and m10, respectively) and pristine PES membrane (45.75%), displaying the better antifouling ability. Much research has revealed that if the hydrophilicity of membrane surface is sufficiently high, the oil adsorption could be reduced remarkably [4,5,7]. In this study, PES membranes were modified by PHEMA-b-F127-b-PHEMA, and the highly hydrated PHEMA chains adsorbed large quantities of water molecules and formed a homogeneous water layer. Thus, the irreversible oil adsorption or deposition was restricted to a lower level, and the flux could be mostly recovered after water washing.

To further analyze the membrane fouling in detail, the  $R_r$ ,  $R_{ir}$  and  $R_i$  values of fabricated membranes were calculated and are listed in Table 2. The pristine PES membrane

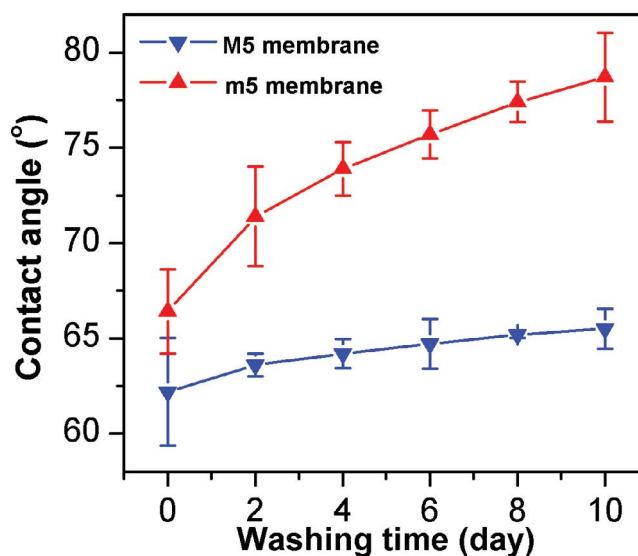


Fig. 14. Water contact angle of m5 and M5 membranes after shaken in water for some time.

has the highest  $R_i$  (82.70%), indicating that the PES membrane suffered a severe permeation flux decline that resulted from the oil fouling. As for the m membrane, the  $R_i$  for m2 reached 62.81% and those for m5, m10 reduced to 58.20%, 56.16%, respectively. It was worth noting that the  $R_i$  of M membranes was evidently lower than m membrane. Furthermore, the percentage of reversible fouling in total fouling ( $R_r/R_i$ ) increased and reached to a maximum (59.36%) when PHEMA-b-F127-b-PHEMA dosage was 10 wt.%, which was higher than that of m10 (55.89%) and pristine PES membrane (34.40%), indicating the reversible fouling plays a vital role in permeation flux decline and the flux can be recovered quickly by hydraulic cleaning [31].

### 3.6. Stability of the additive in the composite membranes

The stability of the additive is a vital factor affecting the lifespan of membrane, which can be detected by measuring the water contact angle of the membrane surface before and after shaking [31]. In this present study, the composite membranes of m5 and M5 were chosen, which were immersed into deionized water under continuous shaking at 50°C for different time spans (2, 4, 6, 8, 10 d). As

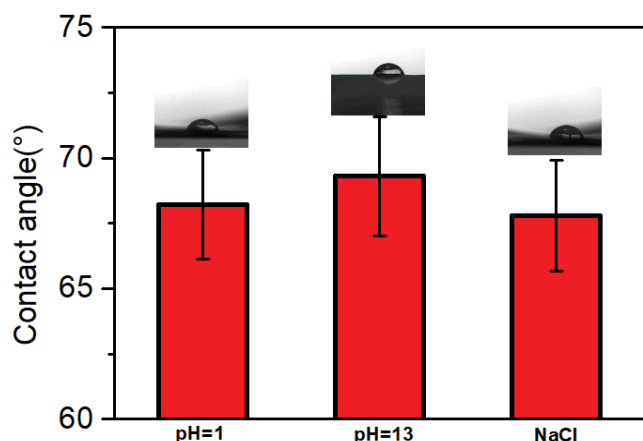


Fig. 15. The water contact angle of M5 membrane after washed with aqueous solutions at pH = 1, pH = 13 and 1 M NaCl for 10 d.

presented in Fig. 14, the membrane surface contact angle gradually increased with the increase of the shaking time. The contact angle of the fresh m5 membrane (shaking for 0 d) was  $66.4^\circ \pm 2.2^\circ$ . After continuously shaking for 10 d, the contact angle increased 18.5% and reached  $78.7^\circ \pm 2.3^\circ$ . As for M5 membrane, the water contact angle after shaking 10 d ( $65.5^\circ \pm 1.1^\circ$ ) was slightly higher than that of the fresh membrane ( $62.2^\circ \pm 2.8^\circ$ ), which increased 5.2% only, displaying the better stability.

Furthermore, the water contact angles of M5 membrane after washed with different aqueous solutions (pH = 1, pH = 13 and 1 M NaCl) for 10 d are shown in Fig. 15. As shown in Fig. 15, the water contact angles had a little variation after shaking 10 days of different aqueous solutions ( $68.2^\circ$ ,  $69.3^\circ$  and  $67.8^\circ$  for pH = 1, pH = 13 and 1 M NaCl, respectively), suggesting the excellent stability of the PES/FH composite membrane.

#### 4. Conclusions

The incorporation of copolymer PHEMA-b-F127-b-PHEMA containing reactive PHEMA chains into PES membranes offered a possibility to improve the hydrophilicity and antifouling properties of PES membranes. The hydrophilic PHEMA chains in the copolymer additive were concentrated onto the fabricated membrane surface due to the surface segregation phenomenon in the NIPS process. Furthermore, the PHEMA chains enriched on the PES composite membrane surface, which could act as an anchor to immobilize the initiating site. Therefore a lot of functional polymers would effectively graft onto the PES composite membranes by surface-initiated radical polymerization, which provides a facile technology for designing and fabricating antifouling advanced membranes.

#### Acknowledgment

The authors are grateful for the financial supports from the Jiang xi Provincial Sci & Tech Plan of China (Grant No. GJJ202805) and Jing de Zhen Sci & Tech Plan of China (Grant No.2017GYZD021-03).

#### References

- [1] M.A. Shannon, P.W. Bohn, M. Elimelech, J.G. Georgiadis, B.J. Mariñas, A.M. Mayes, Science and technology for water purification in the coming decades, *Nature*, 452 (2008) 301–310.
- [2] D. Sarkar, D. Datta, D. Sen, C. Bhattacharjee, Simulation of continuous stirred rotating disk-membrane module: an approach based on surface renewal theory, *Chem. Eng. Sci.*, 66 (2011) 2554–2567.
- [3] A. Rezvanpour, R. Roostaazad, M. Hesampour, M. Nyström, C. Ghotbi, Effective factors in the treatment of kerosene–water emulsion by using UF membranes, *J. Hazard. Mater.*, 16 (2009) 1216–1224.
- [4] J. Yin, J.C. Zhou, Novel polyethersulfone hybrid ultrafiltration membrane prepared with  $\text{SiO}_2$ -g-(PDMAEMA-co-PDMAPS) and its antifouling performances in oil-in-water emulsion application, *Desalination*, 365 (2015) 46–56.
- [5] W.J. Chen, Y.L. Su, J.M. Peng, X.T. Zhao, Z.Y. Jiang, Y.N. Dong, Y. Zhang, Y.G. Liang, J.Z. Liu, Efficient wastewater treatment by membranes through constructing tunable antifouling membrane surfaces, *Environ. Sci. Technol.*, 45 (2011) 6545–6552.
- [6] J. Yin, H.J. Fan, J.C. Zhou, Cellulose acetate/poly(vinyl alcohol) and cellulose acetate/crosslinked poly(vinyl alcohol) blend membranes: preparation, characterization, and antifouling properties, *Desal. Water Treat.*, 57 (2016) 10572–10584.
- [7] W.J. Chen, J.M. Peng, Y.L. Su, L.L. Zheng, L.J. Wang, Z.Y. Jiang, Separation of oil/water emulsion using Pluronic F127 modified polyethersulfone, *Sep. Purif. Technol.*, 66 (2009) 591–597.
- [8] B. Van der Bruggen, Chemical modification of polyethersulfone nanofiltration membranes: a review, *J. Appl. Polym. Sci.*, 114 (2009) 630–642.
- [9] V. Vatanpour, S.S. Madaeni, L. Rajabi, S. Zinadini, A.A. Derakhshan, Boehmite nanoparticles as a new nanofiller for preparation of antifouling mixed matrix membranes, *J. Membr. Sci.*, 401–402 (2012) 132–143.
- [10] L. Yu, Y.T. Zhang, B. Zhang, J.D. Liu, H.Q. Zhang, C.H. Song, Preparation and characterization of HPEI-GO/PES ultrafiltration membrane with antifouling and antibacterial properties, *J. Membr. Sci.*, 447 (2013) 452–462.
- [11] S.P. Nunes, M.L. Sforca, K.V. Peinemann, Dense hydrophilic composite membranes for ultrafiltration, *J. Membr. Sci.*, 106 (1995) 49–56.
- [12] D.-G. Kim, H. Kang, S.S. Han, J.-C. Lee, The increase of antifouling properties of ultrafiltration membrane coated by star-shaped polymers, *J. Mater. Chem.*, 22 (2012) 8654–8661.
- [13] B.D. McCloskey, H. Ju, B.D. Freeman, Composite membranes based on a selective chitosan-poly(ethylene glycol) hybrid layer: synthesis, characterization, and performance in oil-water purification, *Ind. Eng. Chem. Res.*, 49 (2009) 366–373.
- [14] M.A. Masuelli, M. Grasselli, J. Marchese, et al., Preparation, structural and functional characterization of modified porous PVDF membranes by  $\gamma$ -irradiation, *J. Membr. Sci.*, 389 (2012) 91–98.
- [15] Y. Chen, Q. Deng, J. Xiao, H. Nie, L. Wu, W. Zhou, B. Huang, Controlled grafting from poly(vinylidene fluoride) microfiltration membranes via reverse atom transfer radical polymerization and antifouling properties, *Polymer*, 48 (2007) 7604–7611.
- [16] A. Rahimpour, S.S. Madaeni, S. Zereskhi, Y. Mansourpanah, Preparation and characterization of modified nano-porous PVDF membrane with high antifouling property using UV photo-grafting, *Appl. Surf. Sci.*, 255 (2009) 7455–7461.
- [17] A. Rahimpour, UV photo-grafting of hydrophilic monomers onto the surface of nano-porous PES membranes for improving surface properties, *Desalination*, 265 (2011) 93–101.
- [18] W.J. Chen, Y.L. Su, L.L. Zheng, L.J. Wang, Z.Y. Jiang, The improved oil/water separation performance of cellulose acetate-graft-polyacrylonitrile membranes, *J. Membr. Sci.*, 337 (2009) 98–105.
- [19] Y.F. Zhao, L.P. Zhu, Z. Yi, B.K. Zhu, Y.Y. Xu, Improving the hydrophilicity and fouling-resistance of polysulfone

- ultrafiltration membranes via surface zwitterionization mediated by polysulfone-based triblock copolymer additive, *J. Membr. Sci.*, 440 (2013) 40–47.
- [20] Y.F. Zhao, L.P. Zhu, Z. Yi, B.K. Zhu, Y.Y. Xu, Zwitterionic hydrogel thin films as antifouling surface layers of polyethersulfone ultrafiltration membranes anchored via reactive copolymer additive, *J. Membr. Sci.*, 470 (2014) 148–158.
- [21] Y.F. Zhao, P.B. Zhang, J. Sun, C.J. Liu, Z. Yi, L.P. Zhu, Y.Y. Xu, Versatile antifouling polyethersulfone filtration membranes modified via surface grafting of zwitterionic polymers from a reactive amphiphilic copolymer additive, *J. Colloid Interface Sci.*, 448 (2015) 380–388.
- [22] J.F. Hester, P. Banerjee, Y.Y. Won, A. Akthakul, M.H. Acar, A.M. Mayes, ATRP of amphiphilic graft copolymers based on PVDF and their use as membrane additives, *Macromolecules*, 35 (2002) 7652–7661.
- [23] R. Fan, S.Q. Nie, W.F. Zhao, J. Li, B.H. Su, S.D. Sun, C.S. Zhao, Biocompatibility of modified polyethersulfone membranes by blending an amphiphilic triblock co-polymer of poly(vinyl pyrrolidone)-b-poly(methyl methacrylate)-b-poly(vinyl pyrrolidone), *Acta Biomater.*, 7 (2011) 3370–3381.
- [24] H.M. Song, F. Ran, H.L. Fan, X.Q. Niu, L. Kang, C.S. Zhao, Hemocompatibility and ultrafiltration performance of surface-functionalized polyethersulfone membrane by blending comb-like amphiphilic block copolymer, *J. Membr. Sci.*, 471 (2014) 319–327.
- [25] F. Ran, J.Y. Wu, X.Q. Niu, D. Li, C.X. Nie, R. Wang, W.F. Zhao, W.J. Zhang, Y.H. Chen, C.S. Zhao, A new approach for membrane modification based on electrochemically mediated living polymerization and self-assembly of *N-tert*-butyl amide- and  $\beta$ -cyclodextrin-involved macromolecules for blood purification, *Mater. Sci. Eng., C*, 95 (2019) 122–133.
- [26] M.A.M. Oliveira, C. Boyer, M. Nele, J.C. Pinto, P.B. Zetterlund, T.P. Davis, Synthesis of biodegradable hydrogel nanoparticles for bioapplications using inverse miniemulsion RAFT polymerization, *Macromolecules*, 44 (2011) 7167–7175.
- [27] S. Zhao, Z. Wang, X. Wei, B.R. Zhao, J.X. Wang, S.B. Yang, S.C. Wang, Performance improvement of polysulfone ultrafiltration membrane using PANiEB as both pore forming agent and hydrophilic modifier, *J. Membr. Sci.*, 385–386 (2011) 251–262.
- [28] V. Vatanpour, S.S. Madaeni, R. Moradian, S. Zinadini, B. Astinchap, Novel antibifouling nanofiltration polyethersulfone membrane fabricated from embedding  $\text{TiO}_2$  coated multiwalled carbon nanotubes, *Sep. Purif. Technol.*, 90 (2012) 69–82.
- [29] Q. Yang, Z.K. Xu, Z.W. Dai, J.L. Wang, M. Ulbricht, Surface modification of polypropylene microporous membranes with a novel glycopolymer, *Chem. Mater.*, 17 (2005) 3050–3058.
- [30] X.F. Wang, X.M. Chen, K. Yoon, D.F. Fang, B.S. Hsiao, B. Chu, High flux filtration medium based on nanofibrous substrate with hydrophilic nanocomposite coating, *Environ. Sci. Technol.*, 39 (2005) 7684–7691.
- [31] L.J. Zhu, L.P. Zhu, L.H. Jiang, Z. Yi, Y.F. Zhao, B.K. Zhu, Y.Y. Xu, Hydrophilic and antifouling polyethersulfone ultrafiltration membranes with poly(2-hydroxyethyl methacrylate) grafted silica nanoparticles as additive, *J. Membr. Sci.*, 451 (2014) 157–168.